

## Additional Members of the Local Group of Galaxies and Quantized Redshifts within the Two Nearest Groups

Halton Arp *Max-Planck-Institut für Physik und Astrophysik, Institut für Astrophysik, Karl-Schwarzschild-Str. 1, 8046 Garching bei München, FRG*

Received 1986 November 7; accepted 1987 May 6

**Abstract.** Galaxies of redshift  $z \lesssim 1000 \text{ km s}^{-1}$  are investigated. In the South Galactic Hemisphere there are two large concentrations of these galaxies. One is in the direction of the centre of the Local Group, roughly aligned with M 31 and M 33. The other concentration is centred almost 80 degrees away on the sky and involves the next nearest galaxies to the Local Group, NGC 55, NGC 300 and NGC 253.

The large scale and isolation of these concentrations, and the continuity of their redshifts require that they are all galaxies at the same, relatively close distance of the brightest group members. The fainter members of the group have higher redshifts, mimicking to some extent a Hubble relation. But if they are all at the same average distance the higher redshifts must be due to a cause other than velocity.

The redshifts of the galaxies in the central areas of these groups all obey a quantization interval of  $\Delta cz_0 = 72.4 \text{ kms}^{-1}$ . This is the same quantization found by William Tifft, and later by others, in all physical groups and pairs which have been tested. The quantization discovered here, however, extends over a larger interval in redshift than heretofore encountered.

The majority of redshifts used in the present analysis are accurate to  $\pm 8 \text{ km s}^{-1}$ . The deviation of those redshifts from multiples of  $72.4 \text{ km s}^{-1}$  averages  $\pm 8.2 \text{ km s}^{-1}$ . The astonishing result, however, is that for those redshifts which are known more accurately, the deviation from modulo 72.4 drops to a value between 3 and 4  $\text{km s}^{-1}$ ! The amount of relative velocity allowed these galaxies is therefore implied to be less than this extremely small value.

*Key words:* redshifts, quantization—galaxies, Local Group—galaxies, Sculptor Group

### 1. Introduction

The Local Group, being the closest group to us in space, includes the galaxies we know the most about. However, one strange aspect of the Local Group has emerged over the last decades. That is, with the commonly accepted membership, Local Group galaxies only exhibit a range in redshift of a little over  $200 \text{ km s}^{-1}$  [ $cz_0$  (M 31) =  $-86$  to  $cz_0$  (NGC404) =  $+142 \text{ km s}^{-1}$ ]. Other groups of galaxies characteristically exhibit

redshift ranges of  $800 \text{ km s}^{-1}$  or more. (Jaakkola & Moles 1976; Arp 1982, Fig. 1; Huchra & Geller 1982; Sulentic 1984; Arp & Sulentic 1985; Arp 1986b).

Where are those additional Local Group members which should be present? In order to know where to look we note that in all other groups the less luminous galaxies tend to have the higher redshifts. This is strongly true even within the restricted redshift range of the conventional Local Group. Therefore we would naturally look for the additional members among fainter, higher redshift galaxies. It is clear in any case that no lower redshifts are known which could be candidates for the additional members. Even galaxies with redshifts appreciably higher than  $cz_0 = 142 \text{ km s}^{-1}$  are very scarce. We will therefore see that it is easy to distinguish them from more distant background galaxies.

We make the same kind of analysis of the next nearest group to us in space, the Sculptor Group, and find confirmatory results. Finally we investigate quantization in the redshifts of the galaxies in these groups.

## 2. Distribution of galaxies with $cz_0 < 1000 \text{ kms}^{-1}$ in South Galactic Hemisphere

Table 1 lists all the galaxies known to the author between  $17^{\text{h}} < \text{R. A.} < 5^{\text{h}}$ . They have been gathered from two sources:

- 1) The Revised Shapley Ames Catalog (RSA) by Sandage & Tamman (1981).
- 2) The Rood Catalog (1980), (H. J. Rood, personal communication).

The RSA lists all galaxies brighter than about apparent magnitude 13 and therefore galaxies likely to have the kind of low redshifts we are considering. The Rood Catalog includes the hydrogen line surveys that detect low redshift galaxies to extremely faint apparent magnitudes (particularly the Fisher-Tully surveys). If any additional galaxies turn up in this redshift range in the future they are likely not to have hydrogen and therefore likely not to have redshifts measurable to a sufficient accuracy for the uses of most of the present analysis.

### 2.1 Additional Members of the Local Group of Galaxies

The filled symbols in Fig. 1 represent the traditional members that make up the Local Group. Also plotted in the figure are all the galaxies known in the pictured area which have redshifts slightly above the redshifts of the presently accepted group members. It is clear that the eight additional galaxies with  $300 < cz_0 < 600 \text{ km s}^{-1}$  show a conspicuous concentration just in the Local Group direction.

It would be an unlikely coincidence if a background cluster of galaxies accidentally occurred in this exact region of sky. Moreover we will see that the kinds of galaxies involved are not like those in conventional, more distant clusters. Finally we shall see that this concentration consists of galaxies with not one characteristic redshift. Instead it is made up of a range of redshifts running from the value accepted for members of the Local Group to the  $\Delta cz_0 \simeq 800 \text{ km s}^{-1}$  or more that we would expect to be included in a normal group.

**Table 1.** Galaxies with  $cz_0 < 1000 \text{ km s}^{-1}$   $17^h < \text{R. A.} < 5^h$  (corrected for solar motion of  $\Delta v = 251 \sin l \cos b - 20 \cos l \cos b - 5 \sin b$ ).

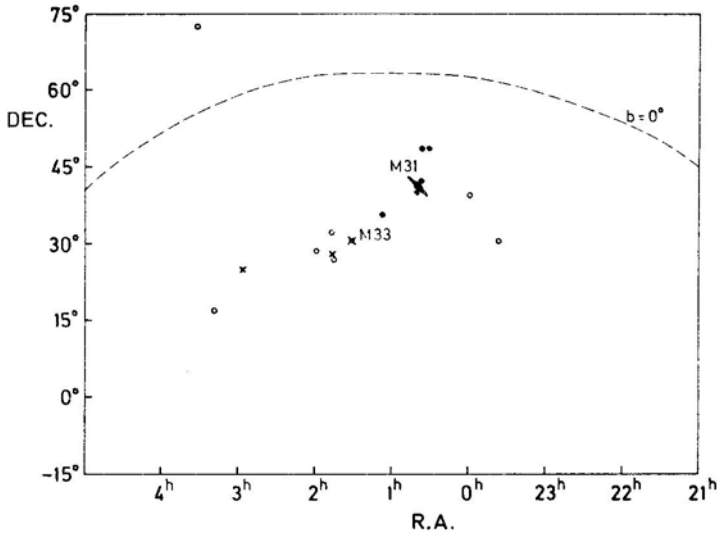
| Galaxy    | R.A. |      | Dec. |    | $cz$<br>$\text{km s}^{-1}$ | $\Delta v$<br>$\text{km s}^{-1}$ | $cz_0$<br>$\text{km s}^{-1}$ |
|-----------|------|------|------|----|----------------------------|----------------------------------|------------------------------|
|           | h    | m    | °    |    |                            |                                  |                              |
| UGC 10669 | 17   | 00.7 | +70  | 22 | $440 \pm 8$                | 203                              | 643                          |
| 10736     | 17   | 08.4 | 69   | 33 | $491 \pm 8$                | 204                              | 695                          |
| 11000     | 17   | 47.7 | 36   | 09 | $300 \pm 167$              |                                  |                              |
| NGC 6689  | 18   | 35.4 | 70   | 29 | $487 \pm 8$                | 221                              | 708                          |
| 6946      | 20   | 33.8 | 59   | 59 | $48 \pm 2$                 | 246                              | 294                          |
| DDO 210   | 20   | 44.2 | -13  | 02 | $-132 \pm 8$               | (150)                            | (18)                         |
| UGC 11891 | 22   | 01.5 | 43   | 30 | $461 \pm 8$                | 249                              | 710                          |
| IC 5201   | 22   | 18.3 | -46  | 19 | $(915 \pm 8)$              | -32                              | 883                          |
| DDO 215   | 22   | 36.5 | -5   | 02 | $829 \pm 8$                | (117)                            | 946                          |
| NGC 7424  | 22   | 54.5 | -41  | 21 | $951 \pm 8$                | -15                              | 936                          |
| 7412 A    | 22   | 54.3 | -43  | 05 | $938 \pm 8$                | -15                              | 923                          |
| 7457      | 22   | 58.6 | 29   | 53 | $525 \pm 90$               |                                  |                              |
| NGC 7640  | 23   | 19.7 | 40   | 34 | $368 \pm 7$                | 236                              | 604                          |
| UGC 12588 | 23   | 22.3 | 41   | 04 | $425 \pm 8$                | 235                              | 660                          |
| —         | 23   | 24.2 | -37  | 37 | $690 \pm 8$                | (-4)                             | (686)                        |
| DDO 216   | 23   | 26.0 | 14   | 28 | $-178 \pm 8$               | 186                              | 8                            |
| DDO 217   | 23   | 27.6 | 40   | 43 | $424 \pm 8$                | 234                              | 658                          |
| IC 5332   | 23   | 31.8 | -36  | 22 | $707 \pm 8$                | -2                               | 705                          |
| NGC 7713  | 23   | 33.6 | -38  | 13 | $698 \pm 8$                | -15                              | 683                          |
| UGC 12713 | 23   | 35.7 | 30   | 26 | $289 \pm 8$                | 218                              | 507                          |
| 12732     | 23   | 38.1 | 25   | 57 | $756 \pm 8$                | 209                              | 965                          |
| —         | 23   | 41.4 | -32  | 15 | $267 \pm 8$                | (17)                             | (284)                        |
| NGC 7741  | 23   | 41.4 | 25   | 48 | $750 \pm 8$                | 208                              | 958                          |
| 7793      | 23   | 55.3 | -32  | 51 | $217 \pm 8^a$              | 5                                | 222                          |
| UGC 12894 | 23   | 57.9 | 39   | 14 | $339 \pm 8$                | 224                              | 563                          |
| DDO 221   | 23   | 59.2 | -15  | 45 | $-124 \pm 8$               | (80)                             | -44                          |
| NGC 24    | 00   | 07.4 | -25  | 15 | $561 \pm 8$                | 22                               | 583                          |
| 45        | 00   | 11.4 | -23  | 27 | $463 \pm 3$                | 37                               | 500                          |
| 55        | 00   | 12.4 | -39  | 28 | $129 \pm 3$                | -28                              | 101                          |
| IC 10     | 00   | 17.6 | 59   | 02 | $-348 \pm 8$               |                                  |                              |
| UGC 290   | 00   | 26.5 | 15   | 37 | $763 \pm 23$               | 166                              | 929                          |
| NGC 147   | 00   | 30.5 | 48   | 14 | $-168 \pm 10^b$            | 222                              | 54                           |
| NGC 185   | 00   | 36.2 | 48   | 04 | $-208 \pm 10^b$            | 220                              | 12                           |
| NGC 205   | 00   | 37.6 | 41   | 25 | $-239 \pm 11$              | 213                              | -26                          |
| M 32      | 00   | 40.0 | 40   | 36 | $-200 \pm 6$               | 211                              | 11                           |
| M 31      | 00   | 40.0 | 41   | 00 | $-297 \pm 0.4$             | 211                              | -86                          |
| IC 1574   | 00   | 40.7 | -22  | 31 | $361 \pm 8$                | 31                               | 392                          |
| NGC 247   | 00   | 44.6 | -21  | 01 | $156 \pm 4$                | 31                               | 187                          |
| 253       | 00   | 45.8 | -25  | 34 | $245 \pm 5$                | 14                               | 259                          |
| DDO 6     | 00   | 47.4 | -21  | 16 | $303 \pm 8$                | 31                               | 334                          |
| NGC 278   | 00   | 49.2 | 47   | 17 | $640 \pm 8$                | 215                              | 855                          |
| NGC 300   | 00   | 52.2 | -37  | 57 | $145 \pm 2$                | -37                              | 108                          |
| IC 1613   | 01   | 02.4 | 01   | 53 | $-238 \pm 90$              |                                  |                              |
| UGC 672   | 01   | 03.3 | 44   | 43 | $712 \pm 8$                | 207                              | 919                          |
| NGC 404   | 01   | 06.7 | 35   | 27 | $-50 \pm 10$               | 192                              | 142                          |
| DDO 9     | 01   | 07.7 | 49   | 20 | $639 \pm 8$                | 215                              | 854                          |
| DDO 10    | 01   | 18.6 | 12   | 09 | $646 \pm 8$                | 129                              | 775                          |
| M 33      | 01   | 31.1 | 30   | 24 | $-180 \pm 0.5$             | -170                             | -10                          |
| NGC 625   | 01   | 32.9 | -41  | 40 | $404 \pm 8$                | -68                              | 336                          |
| NGC 628   | 01   | 34.0 | 15   | 32 | $656 \pm 2$                | 130                              | 786                          |

Table 1. Continued.

| Galaxy       | R.A. |      | Dec. |    | $cz$<br>km s <sup>-1</sup> | $\Delta v$<br>km s <sup>-1</sup> | $cz_0$<br>km s <sup>-1</sup> |
|--------------|------|------|------|----|----------------------------|----------------------------------|------------------------------|
|              | h    | m    | °    | '  |                            |                                  |                              |
| DDO 13       | 01   | 37.5 | 15   | 39 | 634 ± 8                    | 128                              | 762                          |
| UGC 1195     | 01   | 39.7 | 13   | 43 | 767 ± 8                    | 122                              | 889                          |
| NGC 660      | 01   | 40.3 | 13   | 23 | 856 ± 8                    | 120                              | 976                          |
| —            | 01   | 40.6 | 19   | 44 | 501 ± 8                    | 134                              | 635                          |
| A 143        | 01   | 42.9 | -43  | 50 | 394 ± 8                    | (-86)                            | 326                          |
| IC 1727      | 01   | 44.7 | 27   | 05 | 339 ± 8                    | 155                              | 494                          |
| NGC 672      | 01   | 45.0 | 27   | 11 | 413 ± 6                    | 155                              | 568                          |
| UGC 1281     | 01   | 46.7 | 32   | 20 | 163 ± 8                    | 163                              | 326                          |
| NGC 746      | 01   | 54.8 | 44   | 41 | 712 ± 8                    | 185                              | 897                          |
| 784          | 01   | 58.4 | 28   | 35 | 201 ± 8                    | 158                              | 359                          |
| UGC 1561     | 02   | 01.3 | 23   | 58 | 595 ± 8                    | 126                              | 721                          |
| 1807         | 02   | 18.0 | 42   | 32 | 631 ± 8                    | 170                              | 801                          |
| NGC 891      | 02   | 19.3 | 42   | 07 | 530 ± 4                    | 169                              | 699                          |
| DDO 19       | 02   | 21.9 | 35   | 49 | 577 ± 8                    | 154                              | 731                          |
| NGC 925      | 02   | 24.3 | 33   | 22 | 554 ± 8                    | 148                              | 702                          |
| 949          | 02   | 27.8 | 36   | 55 | 610 ± 8                    | 154                              | 764                          |
| 959          | 02   | 29.3 | 35   | 17 | 609 ± 8                    | 149                              | 758                          |
| DDO 22       | 02   | 29.8 | 38   | 28 | 570 ± 8                    | 156                              | 726                          |
| DDO 25       | 02   | 30.3 | 33   | 17 | 611 ± 8                    | 144                              | 755                          |
| DDO 24       | 02   | 30.6 | 40   | 19 | 581 ± 8                    | 160                              | 741                          |
| UGC 2082     | 02   | 33.4 | 25   | 13 | 710 ± 8                    | 121                              | 831                          |
| NGC 1003     | 02   | 36.1 | 40   | 40 | 626 ± 8                    | 158                              | 784                          |
| NGC 1023     | 02   | 37.2 | 38   | 51 | (600 ± 16)                 | 153                              | 753                          |
| 1036         | 02   | 37.6 | 19   | 05 | (787 ± 27)                 | 101                              | 888                          |
| 1058         | 02   | 40.2 | 37   | 08 | 520 ± 8                    | 148                              | 668                          |
| UGC 2259     | 02   | 44.8 | 37   | 20 | 589 ± 8                    | 146                              | 735                          |
| 2432         | 02   | 54.8 | 09   | 55 | 762 ± ?                    | 61                               | 823                          |
| NGC 1156     | 02   | 56.8 | 25   | 03 | 374 ± 8                    | 106                              | 480                          |
| NGC 1291     | 03   | 15.5 | -41  | 19 | 839 ± 4                    | -118                             | 721                          |
| UGC 2684     | 03   | 17.7 | 17   | 08 | 357 ± 8                    | 64                               | 426                          |
| NGC 1343 pec | 03   | 32.4 | 72   | 24 | 300 ± 114                  |                                  |                              |
| IC 342 Sc    | 03   | 42.0 | 67   | 57 | 25 ± 8                     | 178                              | 203                          |
| —            | 03   | 55.0 | 66   | 59 | 72 ± 8                     | 176                              | 248                          |
| NGC 1493     | 03   | 55.9 | -46  | 21 | 1059 ± 8                   | -150                             | 909                          |
| 1507         | 04   | 01.9 | -02  | 19 | 864 ± 8                    | -27                              | 837                          |
| 1512         | 04   | 02.3 | -43  | 29 | 911 ± 8                    | -147                             | 764                          |
| 1569 Irr     | 04   | 26.1 | 64   | 45 | -90 ± 8                    | 161                              | 71                           |
| 1560 Sdm     | 04   | 27.1 | 71   | 48 | -28 ± 8                    | 173                              | 145                          |
| —            | 04   | 27.4 | 63   | 30 | -104 ± 8                   | (161)                            | 57                           |
| NGC 1637     | 04   | 38.9 | -2   | 56 | 726 ± 8                    | -54                              | 672                          |
| DDO 34       | 04   | 46.0 | 0    | 09 | 669 ± 8                    | -48                              | 621                          |
| NGC 1679     | 04   | 48.1 | -32  | 04 | 1059 ± 8                   | (-155)                           | 904                          |
| IC 396       | 04   | 52.8 | 68   | 14 | 762 ± 137                  |                                  |                              |
| NGC 1744     | 04   | 57.9 | -26  | 06 | 742 ± 8                    | -136                             | 606                          |

<sup>a</sup> Redshifts marked thus, or with less than + 8 km s<sup>-1</sup> estimated error have been taken from RSA (Sandage & Tamman 1981)

<sup>b</sup> Redshifts taken from Ford, Jacoby & Jenner (1977) but there is a systematic uncertainty of 10 km s<sup>-1</sup> in their measures. RSA values for  $v_0$  give  $\Delta z_0$  (N 147) = 148 and  $\Delta cz_0$  (N185) = 79. In view of value given in RSA. NGC 185 particularly should be remeasured as accurately as possible.



**Figure 1.** Conventional members of the Local Group ( $-86 \leq cz_0 \leq 142 \text{ km s}^{-1}$ ) are plotted as filled symbols (IC 10 and IC 1613 omitted). Open symbols (dwarfs) and crosses (spirals) represent galaxies from Table 1 which have slightly higher redshifts  $300 < cz_0 < 600 \text{ km s}^{-1}$ .

### 2.2 The M 31–M 33 Line

Additional confirmation that these higher redshift galaxies belong to the Local Group is evident from their linear distribution on the sky, an alignment which coincides very closely with the distribution of the Local Group members. The alignment of the traditionally accepted Local Group members can be seen from the fact that generally along the minor axis direction from M 31 are distributed the smaller companion members in the Local Group: NGC 147, 185, 205, 221, 404, 598, dwarf spheroidals and peculiar H I clouds (Arp 1987). The coincidence of a background cluster being this elongated and also accidentally this well positioned and aligned with the accepted Local Group would seem to be very small.

### 2.3 Testing the Redshift Range of the Members

Fig. 2 plots all the galaxies in the pictured region which have redshifts  $cz_0 < 940 \text{ km s}^{-1}$  (with the exception of IC 10 and IC 1613 which are probably very close to our own Milky Way galaxy). We see there is a tight group at high northern declinations, the NGC 1569–IC 342 group, but in addition, more galaxies in this higher redshift range which are concentrated in the general direction of the Local Group and the M 31–M 33 line.

In Fig. 2 we have outlined an elongated region, slightly larger around M 31 and narrowing slightly along a line through M 33 and to the southeast. In the following Section 3 we show that this area contains galaxies with the most significant redshift quantization. But here we simply justify it as the densest area of galaxies in the investigated redshift range (excluding the tight group around NGC 891).

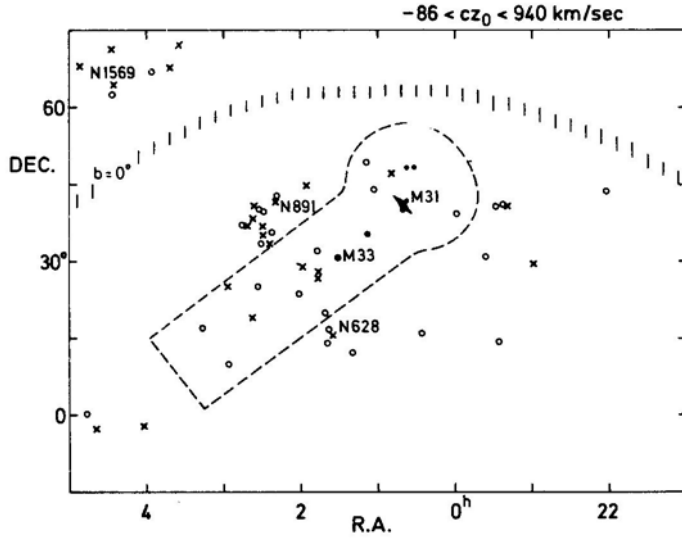


**Figure 2.** All galaxies with  $-86 < cz_0 < 940 \text{ km s}^{-1}$  as listed in Table 1. Symbols are the same as in Fig. 1 except that crosses now represent NGC and IC galaxies, open circles fainter galaxies. Region inside dashed contour is used to test Local Group membership in Fig. 3a and quantization in Fig. 5a.

For the galaxies in this line we now plot Fig. 3a. We see their redshifts are rather evenly spread between  $0 < cz_0 < 900 \text{ km s}^{-1}$ . On the hypothesis that this concentration of galaxies on the sky represented a background group accidentally falling behind the Local Group centre we would expect a peak of redshifts corresponding to that greater distance. Instead we see an even filling in between galaxies of the accepted Local Group redshift and the expected range of a single group membership.

In Fig. 3 the dashed curve shows how numbers of galaxies should increase if they were homogeneously spread through space. The volume sampled should increase as

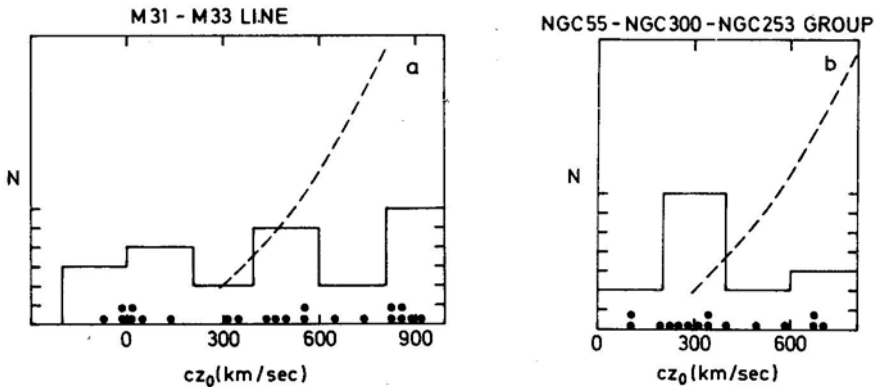


**Figure 3.** Numbers of galaxies as a function of redshift within Local and Sculptor Groups. a) Within dashed boundary in Fig. 2. b) Within dashed boundary in Fig. 4. Dashed curve illustrates how  $N \propto z^3$  (or, in this case how  $dN \propto z^2$ ) would appear.

the cube of the redshift on the redshift-distance assumption. But the observed histograms rule out the possibility that the pictured differential counts increase as  $z^2$ . Therefore we conclude that the concentration of galaxies that we see in Figs 1 and 2 is for the most part physically associated with the Local Group and represents the expected range of redshift membership in a group of about  $0 \lesssim cz_0 \lesssim 900 \text{ km s}^{-1}$ .

#### 2.4 Comment on the Hubble Relation

Table 2 lists the individual galaxies which are considered here to be members of the M 31–M 33 line. It is clear that the fainter galaxies have generally higher redshifts. In this sense they obey a Hubble relation. But if these intrinsically higher redshift galaxies are actually intrinsically less luminous they would still mimic a distance-redshift relation even though all at the same distance. This is unquestionably the case in the galaxies classically considered members of the Local Group ( $-86 \leq cz_0 \leq 142 \text{ km s}^{-1}$ ). Those companions define a quite accurate  $cz_0 \propto 5 \log m$  relation even though they are all at the same distance (Arp 1987). The fainter members included here in the Local Group could follow a loose Hubble relation until apparent magnitude  $\simeq 14$ . Fainter than this the galaxies deviate strongly below a linear Hubble relation. Usually a deviation from a Hubble line is interpreted as a deviation in luminosity. But in fact what it means is that these objects do not themselves define a

**Table 2.** Galaxies in M 31–M 33 line with  $-86 < cz_0 < 1000 \text{ km s}^{-1}$ .

| Galaxy               | R.A.    | Dec.  | $cz_0^a$      | Relative to M 31 |           | mag.  | Type               |
|----------------------|---------|-------|---------------|------------------|-----------|-------|--------------------|
|                      |         |       |               | $\Delta cz_0$    | Mod 72.4  |       |                    |
| UGC 12894            | 23 57.9 | 39 14 | $563 \pm 8$   | 649              | 9–3       | 17    | Irr v              |
| NGC 147              | 00 30.5 | 48 14 | $54 \pm 10^b$ | 140              | 2–5       | 9.96  | dE5                |
| NGC 185              | 00 36.2 | 48 04 | $12 \pm 10^b$ | 98               | 1 + 26    | 9.73  | dE3 pec            |
| NGC 205              | 00 37.6 | 41 25 | $-26 \pm 11$  | 60               | 1–12      | 8.60  | S0/E5 pec          |
| M 32                 | 00 40.0 | 40 36 | $11 \pm 6$    | 97               | 1 + 25    | 8.79  | E2                 |
| M 31                 | 00 40.0 | 41 00 | $-86 \pm 0.4$ | 0                | reference | 3.12  | Sb t-II            |
| NGC 278              | 00 49.2 | 47 17 | $855 \pm 8$   | 941              | 13–0      | 10.85 | Sbc II             |
| UGC 672              | 01 03.3 | 44 43 | $919 \pm 8$   | 1005             | 14–9      | 18    | Irr v              |
| NGC 404              | 01 06.7 | 35 27 | $142 \pm 10$  | 228              | 3 + 11    | 10.96 | SO pec             |
| DDO 9                | 01 07.7 | 49 20 | $854 \pm 8$   | 940              | 13–1      | 17    | Irr v              |
| M 33                 | 01 31.1 | 30 24 | $-10 \pm 0.5$ | 76               | 1 + 4     | 5.6   | Sc II-III          |
| —                    | 01 40.6 | 19 44 | $635 \pm 8$   | 721              | 10–3      |       | Fisher–Tully dwarf |
| IC 1727              | 01 44.7 | 27 05 | $494 \pm 8$   | 580              | 8 + 4     | 12.2  | Irr I              |
| NGC 672              | 01 45.0 | 27 11 | $568 \pm 6$   | 654              | 9 + 2     | 10.69 | SBc III            |
| UGC 1281             | 01 46.7 | 32 20 | $326 \pm 8$   | 412              | 6–22      | 13.0  | S IV?              |
| NGC 784              | 01 58.4 | 28 35 | $359 \pm 8$   | 445              | 6 + 10    | 12.1  | S dm               |
| UGC 1561             | 02 01.3 | 23 58 | $721 \pm 8$   | 807              | 11 + 11   | 14.7  | Irr I              |
| UGC 2082             | 02 33.4 | 25 13 | $831 \pm 8$   | 917              | 13–24     | 14.0  | Sc                 |
| NGC 1036             | 02 37.6 | 19 05 | $888 \pm 27$  |                  |           | 13.5  | pec Mark 370       |
| UGC 2432             | 02 54.8 | 09 55 | $823 \pm ?$   |                  |           | 17    | S v                |
| NGC 1156             | 02 56.8 | 25 03 | $480 \pm 8$   | 566              | 8–13      | 11.92 | Sm v-IV            |
| UGC 2684             | 03 17.7 | 17 08 | $426 \pm 8$   | 512              | 7 + 5     | 18–19 | dwarf?             |
| NGC 628 <sup>c</sup> | 01 34.0 | 15 32 | $786 \pm 2$   | 872              | 12 ± 3    | 9.43  | Sc I               |

<sup>a</sup> Values with errors less than  $\pm 8 \text{ km s}^{-1}$  have been taken from RSA.

<sup>b</sup> see note to Table 1.

<sup>c</sup> Slightly outside slot in Fig. 1 but predicted to be Local Group member (Arp 1986a).

Hubble line and therefore there is no evidence that these particular galaxies are in fact at their redshift distance.

In Table 2 the morphological types of the galaxies in the M 31–M 33 lines are listed. It is evident that they are almost entirely late type spirals or low surface brightness irregulars. This is not the morphological composition of a normal galaxy cluster. Moreover it is just these kinds of galaxies which have been shown to violate redshift-distance relations because of their intrinsic redshifts (Arp 1986b). In general, the one kind of galaxy for which we have some evidence that a true redshift–distance relationship is obeyed, is Hubble type Sb (like M 31 and M 81). This class is completely unrepresented among the higher redshift members of the M 31–M 33 line.

### 2.5 The NGC 55–NGC 300–NGC 253 Group

Fig. 4 shows a plot in the sky at southern declinations of the galaxies from Table 1 in the redshift interval  $100 < cz_0 < 800 \text{ km s}^{-1}$ . This region of the sky includes the well-known Sculptor group of three bright Sc galaxies. Again we see that of all the area possible inside the frame only the region just in the direction of these bright Sculptor spirals is populated by fainter galaxies. As was true of the Local Group, there should be fainter members of the group, and here are the only possible candidates. The Sculptor Group is about 3 times more distant than M 31 and the Local Group, and its apparent diameter on the sky is about 3 times smaller.

Fig. 3b shows the same situation pertains as in the Local Group. The redshifts of the fainter galaxies are not clumped at any particular value but spread evenly between those of the brightest and faintest members. Therefore we see that the Local Group and the next nearest group to us, the Sculptor Group both agree in having companions that range from  $700$  to  $900 \text{ km s}^{-1}$  higher redshift than the dominant galaxies in the group.

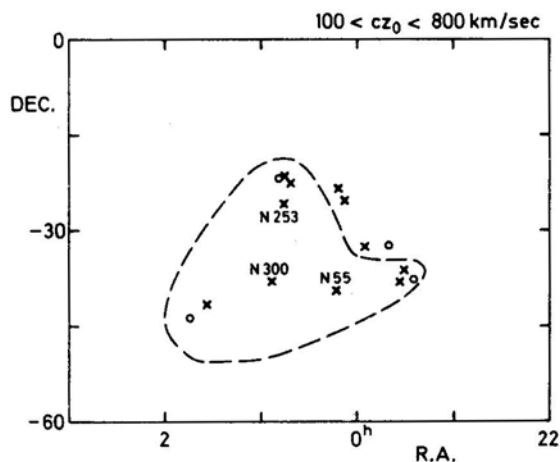


**Figure 4.** All galaxies in indicated redshift range in Sculptor region of sky. Symbols are as in Fig. 2.

### 3. Quantization of redshifts

It was shown originally that Local Group galaxies had redshifts quantized in units of  $72 \text{ km s}^{-1}$  (Tifft 1977). More recently it was shown that the most accurate update of redshifts of companion galaxies in both the traditionally accepted M 31 and M 81 groups were significantly grouped into multiples of  $72.4 \text{ km s}^{-1}$  (Arp 1986a). In order to demonstrate this quantization a correction for solar motion had to be derived and applied which was more accurate than the correction customarily used. (This correction is principally galactic rotation of the Sun around our galactic centre plus a small component of peculiar motion of our Galaxy.) Particularly for members of groups which are seen in appreciably different directions on the sky, the correction must be very exact or it will degrade any existing quantization of relative redshifts between galaxies.

Therefore in Table 1 all measured redshifts of galaxies,  $cz$ , have been corrected by the more accurate formula in the beginning of the table to obtain redshifts relative to the mean of Local Group galaxies, the quantity called  $cz_0$  (see Arp 1986a for derivation of new correction formula). For the Local Group galaxies, Table 2 adds the measured redshift of M 31 ( $86 \text{ km s}^{-1}$ ) to all values of  $cz_0$  to give relative redshifts of the remaining galaxies with respect to M 31.

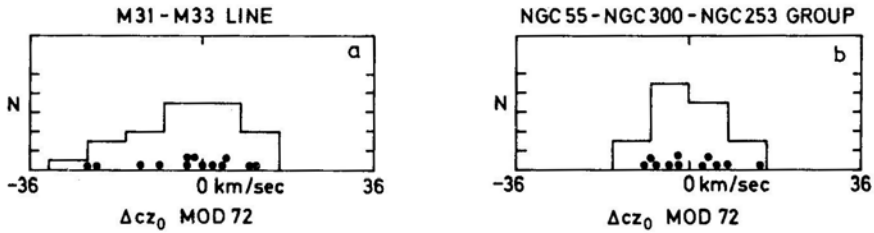
#### 3.1 The M31–M33 Line

Table 2 also lists, for all the galaxies within the area outlined by dashes in Fig. 2, what their relative redshifts are with respect to M 31 in multiples of  $72.4 \text{ km s}^{-1}$ . It is seen that these differential redshifts range all the way from one multiple of  $72.4$  up to almost 14 multiples. But there is remarkably small deviation from the predicted modulo  $72.4$ ! Consider that if the data had no tendency to be quantized, the residuals from mod  $72.4 \text{ km s}^{-1}$  would be randomly spread between  $+36 \text{ km s}^{-1}$  and  $-36 \text{ km s}^{-1}$ .

Fig. 5a shows that those 13 companions within the outlined area of Fig. 2 that have redshifts which are 6 to 14 multiples of  $72.4$ , are with but two exceptions accurately quantized. A very nonrandom concentration of points appears near  $\Delta cz_0 \pmod{72.4} = 0$ . A crude test of the probability of accidentally finding a concentration of 11 out of 13  $\Delta z$ 's within  $\pm 14 \text{ km s}^{-1}$  of  $\Delta z = 0$ , as pictured in Fig. 5a, is  ${}^{11}P_{13} (14/36) \lesssim 10^{-3}$ . Perhaps even more impressive is the fact that Fig. 5 shows that the majority of points fall within  $+8 \text{ km s}^{-1}$  of the multiples of  $72.4 \text{ km s}^{-1}$ . But  $\pm 8 \text{ km s}^{-1}$  is the accuracy of the measured redshifts so they could not average any closer than this. Extensive power spectrum analyses of periodicities in these data are being performed by W. Napier, B. Guthrie & B. Napier (Royal Observatory Edinburgh).\*

In Fig. 5a the lower redshift, traditional members of the Local Group have not been plotted. The reason is that these have already been demonstrated to obey a  $72.4 \text{ km s}^{-1}$  periodicity (Arp 1985). In fact this is where the more accurate value of  $72.4$  was derived rather than the previously used value of  $72$ . The important aspect of Fig. 5a is that *the additional* members of the Local Group identified in Fig. 2 and Table 2 *independently* confirm exactly the same value of quantization as the original Local Group members.

\*See report in "New Ideas in Astronomy", Istituto Veneto di Scienza, Venice, 5–7 May 1987, Eds F. Bertola, B. Madore & J. W. Sulentic.



**Figure 5.** Distribution of residuals from modulus  $72.4 \text{ km s}^{-1}$  for: a) Galaxies with accuracy  $\pm 8 \text{ km s}^{-1}$  or better from Table 2. b) Galaxies inside dashed contour in Fig. 4, also listed in Table 3.

### 3.2 The NGC 55–NGC 300–NGC 253 Group

Table 3 extracts the data on the galaxies pictured in Fig. 4. The mod 72.4 column shows that these Sculptor galaxies are generally shifted in zero point with respect to M 31. But this is to be expected since the Sculptor Group is a separate group from the Local Group and it would be expected that there might be some peculiar motion between the groups, or offset in zero point between the redshift of the two groups. For now we will consider the Sculptor group to be approaching the Local Group with a velocity of  $-34 \text{ km s}^{-1}$ . Adding this velocity to all the Sculptor Group galaxies gives the values listed finally in Table 3. Fig. 5b shows the Sculptor galaxies now have redshifts with only one exception within  $+9 \text{ km s}^{-1}$  of modulo  $72.4 \text{ km s}^{-1}$ .

A dashed line in Fig. 4 outlines a contiguous area within which all the galaxies obey the modulo 72.4 law. Four galaxies are excluded on the edge of this area which have a different zero point for their redshifts. They are excluded from Fig. 5b and listed at the end of Table 3. These four are perfectly quantized with respect to our own Local Group without any correction of  $34 \text{ km s}^{-1}$ . It is not known what significance, if any, this fact has.

**Table 3.** Galaxies in NGC 55–NGC 300–NGC 253 group ( $100 < cz_0 < 800 \text{ km s}^{-1}$ ).

| Galaxy    | R.A.    | Dec.   | $cz_0$      | Mod 72.4 | + 34 $\text{km s}^{-1}$ | $B_T^{0,i}$ | Type               |
|-----------|---------|--------|-------------|----------|-------------------------|-------------|--------------------|
| —         | 23 24.2 | −37 37 | $686 \pm 8$ | 9 + 34   | 10−4                    |             | Fisher–Tully dwarf |
| IC 5332   | 23 31.8 | −36 22 | $705 \pm 8$ | 10−19    | 10+15                   | 10.87       | Sc II–III          |
| NGC 7713  | 23 33.6 | −38 13 | $683 \pm 8$ | 9+13     | 10−7                    | 11.08       | Sc II–III          |
| NGC 55 00 | 12.4    | −39 28 | $101 \pm 3$ | 1+29     | 2−9                     | 7.35        | Sc                 |
| IC 1574   | 00 40.7 | −22 31 | $392 \pm 8$ | 5+30     | 6−8                     |             | Irr                |
| NGC 247   | 00 44.6 | −21 01 | $187 \pm 4$ | 3−30     | 3+4                     | 8.88        | Sc III–IV          |
| NGC 253   | 00 45.1 | −25 34 | $259 \pm 5$ | 4−31     | 4+3                     | 7.38        | Sc                 |
| DDO 6     | 00 47.4 | −21 16 | $334 \pm 8$ | 5−28     | 5+6                     |             | dwarf              |
| NGC 300   | 00 52.5 | −37 57 | $108 \pm 2$ | 1+36     | 2−2                     | 8.31        | Sc II              |
| NGC 625   | 01 32.9 | −41 40 | $336 \pm 8$ | 5−26     | 5+8                     | 11.91       | Im III             |
| A 143     | 01 42.9 | −43 50 | $326 \pm 8$ | 5−36     | 5−2                     | (13.1)      | Irr                |
| —         | 23 41.4 | −32 15 | $284 \pm 8$ | 4−6      |                         |             | Fisher–Tully dwarf |
| NGC 7793  | 23 55.3 | −32 51 | $222 \pm 8$ | 3+5      |                         | 9.25        | Sd IV              |
| NGC 24    | 00 07.4 | −25 15 | $583 \pm 8$ | 8+4      |                         | 11.35       | Sc II–III          |
| NGC 45    | 00 11.4 | −23 27 | $500 \pm 3$ | 7−7      |                         | 11.69       | Scd III            |

In order to test the significance of the quantization in the Sculptor Group we use the largest, low-redshift normal-appearing galaxy in the group, NGC 300, as a redshift reference. This is the same procedure as in the Local Group. Table 3 shows that 9 of the 14 remaining members fall within  $\pm 10 \text{ km s}^{-1}$  of modulo 72.4. This gives a probability of  ${}^9P_{14} = 4 \times 10^{-3}$  that the remaining members would accidentally be quantized this closely with respect to NGC 300. Of course the small subgroup of four galaxies is very tightly grouped in  $\Delta z$  and in a very small area on the edge of the Sculptor Group. If we are allowed to choose the central region of the Sculptor Group as drawn in Fig. 4, the probability of accidental quantization in Fig. 5b is only  ${}^9P_{10} = 7 \times 10^{-5}$ .

### 3.3 How Exact is the Quantization?

For most of the redshifts listed in Tables 2 and 3 the quoted error of determination is  $\pm 8 \text{ km s}^{-1}$ . These are almost entirely values described by Rood as "Very high quality 21 cm redshifts [that] are assigned the nominal (and realistic) value of  $\pm 8 \text{ km s}^{-1}$ ". Fig. 6 shows that if we consider only redshifts with this rms error then the average residual from modulo 72.4 is just  $8.2 \text{ km s}^{-1}$ . We appear to confirm that  $8 \text{ km s}^{-1}$  is actually the accuracy with which these redshifts have been measured.

But now Fig. 6 additionally shows that for 7 redshifts which are known with greater accuracy than  $\pm 8 \text{ km s}^{-1}$ , their residual deviations from modulo 72.4 are dramatically smaller. In fact, Fig. 6 shows that the true accuracy of quantization for the redshifts considered here reaches to within at least  $\pm 3$  to  $\pm 4 \text{ km s}^{-1}$ ! Since peculiar, relative velocities of more than this amount would destroy this accurate quantization, the startling implication is that these groups of galaxies have internal motions that are less than  $\pm 3$  to  $\pm 4 \text{ km s}^{-1}$ !

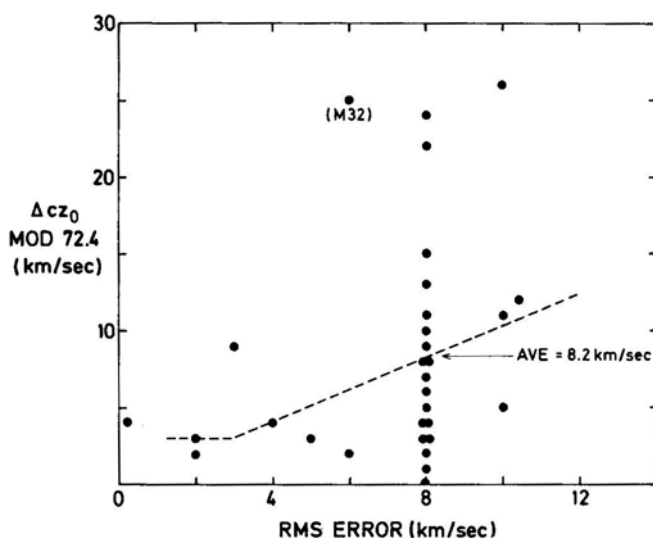


**Figure 6.** Residuals from modulus  $72.4 \text{ km s}^{-1}$  as a function of the rms error of measurement of the redshifts. Average residual for measures which are accurate to  $\pm 8 \text{ km s}^{-1}$  comes out to be  $\pm 8.2 \text{ km s}^{-1}$ . M 32 is discussed in text.

There are two further comments to be made about Fig. 6. First, the one point with accuracy better than  $\pm 8 \text{ km s}^{-1}$  which falls far from modulo 72.4 is M 32. M 32 is so close to the disc of M 31 that it is clearly warping the disc of M 31 (Arp 1964). A gravitational interaction of M 31 and M 32 is therefore implied. This, in turn, would seem to require an appreciable component of relative velocity to be reflected in the redshift of M 32.

Secondly, the one point slightly outside the slot in Fig. 1 which is plotted in Fig. 6 is NGC 628 (added to the bottom of Table 2). NGC 628 is one of the brightest apparent-magnitude Sc spirals in the region and several pieces of evidence placed it as a member of the Local Group (Arp 1986b). Now we see that its accurately measured redshift, compared to the accurate redshift of M 31, confirms to a high accuracy its quantized value of redshift and thus gives quantitative confirmation of its membership in the Local Group.

### 3.4 Remark on the Value of the Hubble Constant, $H_0$

Regardless of whether or not the universe is expanding, the general existence of an apparent-magnitude-redshift relation (the Hubble Relation) for Sb galaxies (Arp 1986b) implies there is a redshift–distance relation in the universe. The Tully–Fisher relation for galaxies (excluding those with intrinsic redshifts) yields,  $H_0 = 55 \text{ km s}^{-1} \text{ Mpc}^{-1}$  (see Arp 1986b, Fig. 10 and accompanying discussion). It is interesting to see how the value of this Hubble constant which everyone has worked so hard to measure fares in a universe which has non-velocity and quantized redshifts.

Table 4 summarizes the situation for the three nearest, major groups of galaxies. The distance modulus for M 31 is taken from the RSA ( $\mu = 24.2 \text{ mag}$ ), as well as the distance modulus for NGC 300 ( $\mu = 26.8 \text{ mag}$ ). For M 81, however, the RSA value of  $\mu = 27.7 \text{ mag}$  was later superseded by a much more distant value of  $\mu = 28.8 \text{ mag}$  (Sandage 1984). However the discussion of M 81 and the Tully–Fisher relation in Arp 1986b indicated an intermediate modulus of  $\mu = 28.0 \text{ mag}$  was more likely. That is the value adopted here although the exact value is not critical to the argument which follows.

The redshift of the dominant galaxies in each group are corrected for the solar motion listed at the head of Table 1 and indicated as  $cz_0$  in the third column of Table 4. Immediately we see that the measured redshifts of these three groups are much too small to give a reasonable  $H_0$  at their known distances. Their average  $H_0$  would actually be negative because of the large negative redshift of M 31. But we know that in order to have M 31 agree with even its most immediate neighbours we must add  $72 \text{ km s}^{-1}$ , one quantization unit, to its measured redshift value. After doing that, and if

**Table 4.** Hubble constant and peculiar velocity for nearest three galaxy groups.

| Galaxy         | distance (Mpc) | $cz_0$   | $H_0$ | after<br>type corr. | $H_0$  | for<br>$H_0$ | required<br>pec vel. |
|----------------|----------------|----------|-------|---------------------|--------|--------------|----------------------|
| M 31           | 0.7            | −86      | −124  | +72                 | −20    | $H_0 = 0$    | −14                  |
| NGC 55–NGC 300 | 2.3            | 101, 108 | 45    | 0                   | 45     | $H_0 = 55$   | −22                  |
| M 81           | 4.0            | 89       | 22    | +72(144)            | 40(59) | $H_0 = 55$   | −58 (+15)            |

$H_0 = 0$  within the Local Group, then M 31 and our own Milky Way Galaxy would have a true differential velocity of only  $-14 \text{ km s}^{-1}$ .

For NGC 55–NGC 300 the measured  $cz_0$  divided by the adopted distance yields  $H_0 = 45$ . If  $H_0$  were actually  $H_0 = 55$ , then NGC 55–NGC 300 would have to have a peculiar velocity of  $-22 \text{ km s}^{-1}$ . But this is nearly the peculiar velocity needed in Section 3.2 to bring the quantization of Sculptor Group into zero point agreement with the quantization of the Local Group redshifts! Since this latter value could have come out anywhere between  $-36$  and  $+36 \text{ km s}^{-1}$ , it is possibly not a coincidence.

Finally the low measured  $cz_0$  and large distance of M 81 yield a pitifully small  $H_0 = 22 \text{ km s}^{-1} \text{ Mpc}^{-1}$  for this important system. But, as in M 31, we must make a type correction of  $72 \text{ km s}^{-1}$  for the dominant Sb (M 81) relative to our Sc (companion type) galaxy. Then the derived  $H_0 = 40 \text{ km s}^{-1} \text{ Mpc}^{-1}$ . If the type correction were two multiples of quantization ( $2 \times 72.4 = 145 \text{ km s}^{-1}$ ) then the  $H_0$  derived from M 81 would be  $H_0 = 59 \text{ km s}^{-1} \text{ Mpc}^{-1}$ . In these two cases the peculiar velocity of M 81 needed to give  $H_0 = 55$  would be reduced from  $-131 \text{ km s}^{-1}$  to  $-59$  or even possibly  $+15 \text{ km s}^{-1}$ . *The bottom line is that if the Hubble constant which is characteristic of extragalactic space is really  $H_0 = 55$ , the corrections to the observed redshifts required by the quantization yields much more believable peculiar motions for the three nearest galaxy groups.*

One comment on the NGC 55–NGC 300 group is that since these two galaxies are type Sc they would not be expected to have any relative quantization correction to our own (approximately) type Sc galaxy. It is just the NGC 55–NGC 300 group which, without correction, gives the most reasonable value of  $H_0 = 45$ .

Another comment is that NGC 253 at about  $154 \text{ km s}^{-1}$  higher redshift in the NGC 55–NGC 300 group is very bright in apparent magnitude. This is reminiscent of the situation with M 82, which is attached by hydrogen bridges to M 81. M 82 is  $+285 \text{ km s}^{-1}$  relative to M 81 but is very bright for such a relatively highly redshifted companion. Like M 82, NGC 253 is an active, ejecting galaxy of peculiar, mottled appearance and very little resolution into stars. It is suggested here that both are fainter, intrinsically redshifted galaxies which are temporarily in a bright phase.

#### 4. Summary and discussion

Quantization of galaxy redshifts was first discovered by Tiftt in 1972. He noticed that redshifts of galaxies in the Coma Cluster when plotted in an apparent-magnitude-redshift diagram formed bands, separated by discrete values of redshift. In 1976 he analyzed individual spiral galaxies and concluded that the discrete redshift interval was between  $70$ – $75 \text{ km s}^{-1}$  (Tiftt 1976). In 1977 he confirmed this quantization in redshifts of double (binary) galaxies. In this same paper, by identifying redshift bands separated by several multiples in the Coma Cluster, he calculated the value  $\text{mod } \Delta cz_0 = 72.46 \text{ km s}^{-1}$  (Tiftt 1977). By 1980 accurate hydrogen redshifts had been measured by others for a new sample of double galaxies and the  $72 \text{ km s}^{-1}$  periodicity was confirmed even more strongly (Tiftt 1980).

The largest and most accurate sample, an independent sample of galaxies in groups, was then reported by Arp & Sulentic (1985). The quantization of  $72 \text{ km s}^{-1}$  was again, inescapably confirmed. Finally, analysis of the most accurate redshifts available in the

close-by M 31 and M 81 groups, with a new and more accurate solar motion correction, yielded a quantization value of  $72.4 \text{ km s}^{-1}$  (Arp 1986a, Fig. 4).

It is this value of 72.4 which has been used in the present analysis and which so accurately fits the observed redshifts. Even up to the large redshift represented by 14 multiples of the mod 72.4 value, the fit is extremely good. The goodness of this fit attests to the accuracy of the number in the last decimal place of the derived quantization value.

It should also be emphasized that the full value of 72.4 was taken from concurring previous analyses and applied as a *prediction* to the present data. The fit of this predicted value is shown in Figs 5a and 5b. *But these are redshifts of galaxies not previously tested for this quantization effect,*

It should be commented that Tift & Cocke (1984) test a model of the universe in which the redshifts are globally quantized. They conclude that a general quantization pertains overall, including between groups, but that the intervals are submultiples of  $72.46 \text{ km s}^{-1}$ . In the present paper I only test quantization within groups. The groups in my sample can have arbitrary relative redshifts or peculiar motions between themselves. Their differential offsets, however, should be smaller than about  $\pm 50 \text{ km s}^{-1}$  in order to agree with a 'quiet' Hubble flow (Tamman, Sandage & Yahil 1980).

As for the cause of the effect, there is as yet no physical theory which will quantitatively account for the redshift periodicity observed. Mathematical descriptions of quantum operators on velocity have been discussed (Cocke 1985; Nieto 1986). But the systematically higher redshifts of fainter galaxies in the M 31 and Sculptor Groups which were demonstrated in the present paper require that redshifts higher than that of the dominant galaxy cannot be due to velocity.

The companion galaxies in each group would have to be receding away from the dominant members of the group just in the direction we happen to be looking. This is a *reductio ad absurdum* and shows the fainter galaxies in each group must have higher redshifts due to some other cause than recessional Doppler shift. This excess redshift for fainter galaxies in groups has been established in many separate investigations over the years with independent samples of galaxies (see for review Arp 1976; Arp & Sulentic 1985; Arp 1982; Arp 1986b, d). The critically important consequence is that the observed excess redshifts cannot be, to any appreciable extent, caused by velocities. If one believes that velocities cannot be quantized then the observed quantization is simply another proof that the redshifts are not velocity redshifts. Moreover, whatever is actually causing the intrinsic redshift could then be quantized.

The combination of intrinsic redshift with its strict quantization points, in My opinion, to the properties of matter which constitute these various galaxies as the causative factor. For example, particle masses might be smaller or clocks run slower in the excess redshift galaxies. But regardless of the physical cause of the intrinsic redshifts, if galaxies in groups can be motionless With respect to each other down to values as small as 3 to 4  $\text{kms}^{-1}$  then all current assumptions about masses of galaxies and masses of clusters of galaxies will have to be reexamined.

Undoubtedly many galaxies and peculiar objects will have to be moved closer after allowance for intrinsic redshift effects. Consequently we will have reduced distances and reduced masses. Perhaps this long overdue reexamination of basic assumptions will yield a smaller universe but one with a larger range in the ages of its constituent matter.

### Acknowledgements

I would like to thank J. E. Wampler and W. G. Tifft for critical reading of the manuscript and helpful suggestions.

### References

- Arp, H. 1964, *Astrophys. J.*, **139**, 1045.  
Arp, H. 1976, in *IAU Coll. 37: L'Evolution des Galaxies et ses Implications Cosmologique*, Eds C. Balkowski & B. E. Westerlund, No. 263, C. N. R. S., Paris, p. 377.  
Arp, H. 1982a, *Astrophys. J.*, **256**, 54.  
Arp, H. 1986a, *Astr. Astrophys.*, **156**, 207.  
Arp, H. 1986b, MPA 236.  
Arp, H. 1986c, in *IAU Symp. 124: Observational Cosmology*, Eds A. Hewitt, G. Burbidge & Li Zhi Fang, D. Reidel, Dordrecht; MPA 265.  
Arp, H. 1987, *Quasars, Redshifts and Controversies*, Interstellar Media, California.  
Arp, H., Sulentic, J. W. 1985, *Astrophys. J.*, **291**, 88.  
Ford, H. C., Jacoby, G., Jenner, D. C. 1977, *Astrophys. J.*, **213**, 318.  
Huchra, J. P., Geller, M. J. 1982, *Astrophys. J.*, **257**, 423.  
Jaakkola, T., Moles, M. 1976, *Astr. Astrophys.*, **53**, 389.  
Sandage, A. R. 1984, *Astr. J.*, **89**, 621.  
Sandage, A. R., Tamman, G. A. 1981, *A Revised Shapely-Ames Catalog of Bright Galaxies*, Carnegie Institution, Washington.  
Sulentic, J. W. 1984, *Astrophys. J.*, **286**, 442.  
Tamman, G. A., Sandage, A., Yahil, A. 1980, *Phys. Scripta*, **21**, 630.  
Tifft, W. G. 1972, *Astrophys. J.*, **175**, 613.  
Tifft, W. G. 1976, *Astrophys. J.*, **206**, 38.  
Tifft, W. G. 1977, *Astrophys. J.*, **211**, 31.  
Tifft, W. G. 1980, *Astrophys. J.*, **236**, 70.  
Tifft, W. G., Cocke, J. 1984, *Astrophys. J.*, **287**, 492.